Amine Catalysis and Spontaneous and Specific Acid Catalyses of the Dienone–Phenol Rearrangement

Allyn R. Becker, David J. Richardson, and Thomas C. Bruice*

Contribution from the Department of Chemistry, University of California at Santa Barbara, Santa Barbara, California 93106. *Received January 31, 1977*

Abstract: The pH–rate profiles for the dienone–phenol rearrangements of spiro[3.5]nona-6,8-dien-5-one (**4**), 6-benzyl-6-methyl-2,4-cyclohexadienone (**5**), spiro[4.5]deca-7,9-dien-6-one (**9**), and 6,6-dimethyl-2,4-cyclohexadienone (**7**) have been determined in aqueous solutions. The rate constants for specific acid catalyzed rearrangements were found to be in the order anticipated from a consideration of migratory aptitudes and the relief of ring strain. The pK_a of the protonated dienone **7** was determined (H_0 scale) to be −4.6. The most A-1 reactive dienones were also found to exhibit a spontaneous rearrangement whose rate constant was not influenced by the concentration of lyate species nor by the presence of acid or base species of buffer. In the case of the most reactive dienone (**4**), rearrangement was found to be catalyzed by amines (primary, secondary, and tertiary, Table II). The product of rearrangement was determined to be 4-indanol (amino indanes were not detected). Catalysis of rearrangement of **4** by all of the amines investigated was found to be first order in amine free base and **4** (i.e., k_N[N][4]). In addition, for 7 of the 15 amines a reaction path first order in **4** and protonated amine (i.e., k_a[NH][**4**]) was found to be present. The mechanism of Scheme IV is proposed.

Catalysis of isomerization reactions brought about by addition of a base followed by its elimination (nucleophilic addition–elimination catalysis) is likely to become of increasing interest. We have recently reported two examples of nucleophilic addition–elimination catalysis. The first[1] involved tertiary amine catalyzed rearrangement of 4-carbo-*tert*-butoxybenzene oxide. Trimethylamine adds to the 3 position of the benzene oxide to provide an intermediate which then undergoes general base (and hydroxide) catalyzed elimination of amine

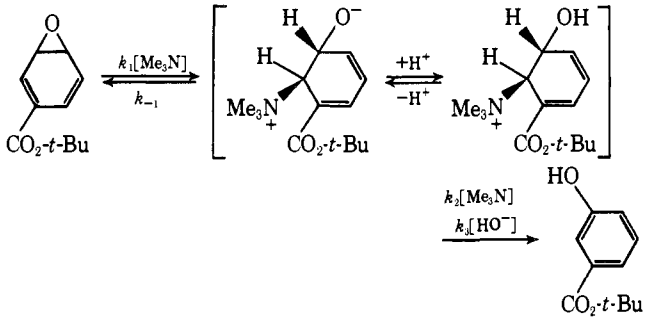

yielding the phenol which is isomeric with starting oxide. This nucleophilic addition–elimination catalysis for arene oxide rearrangement provides an alternate route to the NIH shift. Evidence has recently been presented that an alternate mechanism is prevalent in the hydroxylation of benzenoid hydrocarbons by hepatic monooxygenase.[2] The second example of nucleophilic addition–elimination catalysis was found in the tertiary amine mediated enol–keto tautomerization of oxaloacetic acid (OA) and diethyl oxaloacetate.[3]

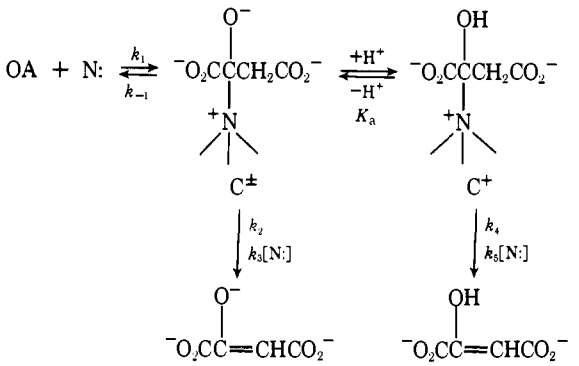

Herein, we report our investigations of the acid-catalyzed, spontaneous, and amine catalysis of the dienone–phenol rearrangement. The dienone rearrangements which have been investigated follow:

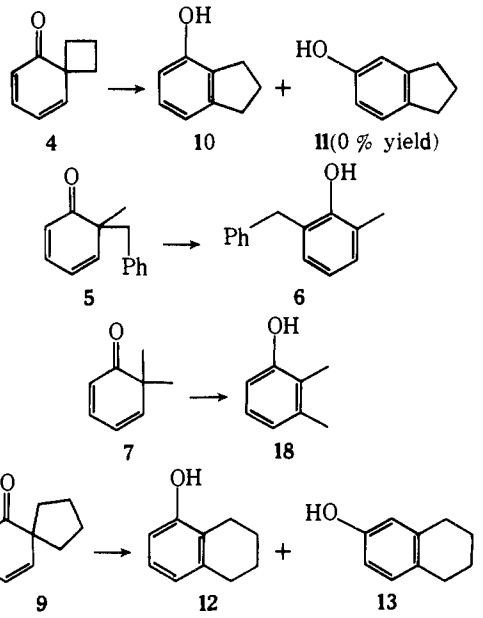

The dienone–phenol rearrangement of spiro[3.5]nona-6,8-dien-5-one (**4**) to provide 4-indanol (**10**) has been found to be catalyzed by ammonia and primary, secondary, and tertiary amines.

Experimental Section

Materials. The hydrochlorides of quinuclidine, dimethylamine, ethylamine, 3-quinuclidinol, trimethylamine, glycine, 3-chloroquinuclidine, Tris (tris(hydroxymethyl)aminomethane), glycinamide, and 3-quinuclidinone were recrystallized from ethanol–water. Pyrrolidine, piperidine, *N*-methylpiperidine, and allylamine were distilled prior to use. The ammonia solutions were titrated against standard hydrochloric acid solutions. The remainder of the buffers were used without further purification. Concentrated solutions of perchloric, hydrochloric, and sulfuric acids were titrated against a standard sodium hydroxide solution.[4] The phenols used for product studies analysis were all obtained from Aldrich and twice sublimed before use. The following melting points were obtained: 4-indanol (**10**), mp 50.7–52.3 °C (lit.[5a] 47–49 °C); 5-indanol (**11**), mp 54.6–56.6 °C (lit.[5b] 51–53 °C); 5,6,7,8-tetrahydro-1-naphthol (**12**), mp 70.8–72.1 °C (lit.[5c] 69–71 °C); and 5,6,7,8-tetrahydro-2-naphthol (**13**), mp 62.0–62.8 °C (lit.[5d] 55–59 °C).

Synthesis. All NMR spectra were obtained on a Varian T-60 spectrometer in carbon tetrachloride with chemical shifts relative to internal Me_4Si. Melting points are uncorrected. Infrared spectra were obtained on a Perkin-Elmer Model 137 infrared spectrophotometer.

Bicyclo[4.3.0]non-3-ene 6-oxide (1) was prepared by a method similar to that used for preparation of 1,2-dimethyl-1,2-epoxycyclohex-4-ene:[6] yellow-green oil, bp 76 °C (9 mm); NMR δ 1.3–2.2 (broad multiplet, 6 H), 2.42 (unresolved multiplet, 4 H), 6.2 (unresolved multiplet, 2 H). ***trans*-3,4-Dibromobicyclo[4.3.0]nonane 6-oxide (2)** was prepared by the method of Wiesel;[7] mp 86–87 °C (lit.[7] mp 87–88 °C). **8,9-Indan oxide (3)** was prepared by the method of Wiesel.[7] The product was obtained pure by distillation at reduced pressure (86–88 °C, 20 mm). The vacuum was released with nitrogen and the collection flask capped immediately: NMR δ 1.2–2.5 (unresolved absorptions, 6 H), 6.21 (broad multiplet, 4 H). **Spiro[3.5]nona-6,8-dien-5-one (4)**, see Kinetic Measurements. **6-Benzyl-6-methyl-2,4-cyclohexadienone (5)** was prepared by the method of Curtin and Wilhelm.[8] The compound was obtained pure after column chromatography (neutral alumina, eluted with hexane–ether (9:1 v/v)) followed by distillation: infrared spectrum showed stretching frequencies at 1670 and 1635 cm^{-1} (lit.[8] 1672 and 1639 cm^{-1}); NMR spectrum agreed with chemical shift assignments by Miller[9] and integrated correctly; UV absorption (cyclohexane solution) showed broad λ_{max} at 297 nm (lit.[8] 298 nm) and a λ_{max} at 312 nm in water where kinetics were performed. **2-Benzyl-6-methylphenol (6)** was isolated from the same reaction which produced **5** following the method of Curtin and Wilhelm.[8] It was recrystallized twice from hexane and sublimed: mp 52.1–53.7 °C (lit.[8] 52 °C); infrared spectrum (KBr pellet) showed broad phenolic absorption at 3350 cm^{-1}; NMR spectrum showed no trace of starting *o*-cresol and integrated correctly, δ 2.2 (singlet, 3 H), 3.9 (singlet, 2 H), 4.4 (singlet, 1 H), 6.8 (complex doublet, 3 H), 7.1 (singlet, 5 H); UV absorption showed λ_{max} at 276 and 267 nm (water solution) while phenolate anion showed λ_{max} at 291 and 240 nm (water solution). **6,6-Dimethyl-2,4-cyclohexadienone (7)** was prepared by the method of Marvell and Magoon.[10] The purified product was obtained by collecting the fraction distilling with bp 84–91 °C (40 mm): NMR δ 1.8 (singlet, 6 H), 6.1 (multiplet, 3 H), 6.9 (multiplet, 1 H); UV absorption showed λ_{max} at 308 nm (typical region for linear conjugated dienones in water solution) with second λ_{max} at 231 nm (lit.[10] 228.5 nm, no solvent listed); in acetonitrile, the dienone showed λ_{max} at 298 and 219 nm; reduction of the dienone with sodium borohydride in water caused disappearance of 308-nm absorption with concomitant formation of product (dienol) at 261 nm (lit.[11] 259 nm in dilute hydrochloric acid). **9,10-Tetralin oxide (8)** was prepared by the method of Wiesel:[7] bp 44 °C (0.30 mm) (lit.[7] 43.5 °C (0.4 mm)); NMR δ 1.5 (multiplet, 4 H), 1.9 (multiplet, 1 H), 2.2 (multiplet, 1 H), 6.1 (singlet, 4 H); ultraviolet absorption shows λ_{max} at 255 nm in ethanol (lit.[7] 259 nm, independent of solvent), and in water **8** shows absorptions (almost immediately) at 314 nm due to rearrangement to dienone **9**.

Spiro[4,5]deca-7,9-dien-6-one (9). As with compound **4**, this compound was generated "in situ" by addition of **8** to water. The λ_{max} occurs at 314 nm. Reduction of **9** with sodium borohydride in water causes loss of 314-nm absorption with a concomitant increase of λ_{max} at 260 nm (compares with dienol produced from **7**).

Kinetic Measurements. All kinetic studies were carried out in deionized and glass-distilled water at 30 °C on a Cary 15, Cary 16, or Cary 118C spectrophotometer. The pH was monitored to ±0.02 unit by use of a Radiometer Model 26 pH meter. The kinetic measurements used for all reactions carried out without buffer at 30 °C (μ = 1.0 with potassium chloride) were obtained in a pH-stat cell designed for the Cary 15 spectrophotometer.[12]

Dienone **4** was generated by adding a small aliquot of a solution of indan oxide (**3**) in acetonitrile to a larger volume of water at pH 7. When the optical density at 317 nm reached a maximum, the formation of **4** was completed.

As an example, buffer dilution experiments with **4** were carried out in the following manner. Dienone **4** was generated by adding 100 μL of a 3.3×10^{-1} M solution of **3** in acetonitrile to 1 mL of 1 M KCl to which had been added 1 drop of KOH. When the absorbance at 317 nm had reached a maximum (ca. 10 min), 200 μL of this solution was then added to each of five cuvettes containing 2.5 mL of the respective buffer at desired pH preequilibrated at 30 °C. The presence of 10^{-4} M EDTA had no effect on the rates of reaction. The formation of phenolic products was followed at pH 14 at 285 nm (λ_{max} of phenolate anion) concomitantly with disappearance of dienone at 317 nm for several runs. All reactions were pseudo-first-order in dienone disappearance or phenol appearance up to 5 half-lives, but were routinely carried out to ca. 2.5 half-lives.

The disappearance of dienone **9** in acid was followed similarly to dienone **4**. Disappearance of dienones **5** and **7** were followed in the acid region by monitoring the decrease in optical density at 312 and 308 nm, respectively. Rearrangements at temperatures much above ambient were carried out in screw cap vials with neoprene-lined caps. The vials were thermostated in an insulated aluminum block. Points were taken by removing vials at regular time intervals and determining the absorbance of the reaction solutions (312, 308, and 314 nm for **5**, **7**, and **9**, respectively). The reactions were found to be first order to greater than 5 half-lives, but were routinely carried out to between 1 and 2 half-lives to maximize absorbance changes. Pseudo-first-order rate constants for all reactions were calculated by least-squares analysis of plots of $\ln (A_\infty - A_0)/(A_\infty - A_t)$ vs. time on a Hewlett-Packard 9820A calculator with a 9862A plotter.

Product Studies. The gas chromatography work was performed on a Hewlett-Packard 5750 gas chromatograph equipped with a thermal conductivity detector. The conditions used for analysis were as follows: column 5 ft × 0.25 in. 20% Apiezon L on Chromosorb W, oven temperature 200 °C, injection port temperature 225 °C, and detector temperature 260 °C. The spectrophotometric determinations were performed on a Cary 118C spectrophotometer. The high-pressure liquid chromatography work employed an Altex Model 100 solvent metering system with a Lichrosorb (Altex) reverse phase column (2.1 × 250 mm) run at room temperature. The flow rate was 0.25 mL/min with a 20% aqueous methanol solvent system for dienone **4** and 0.5 mL/min with a 12% aqueous methanol solvent system for dienone **9**. A Schoeffel SF 7700 spectroflow detector was used in conjunction with a recorder and Varian CDS 101 integrator.

Search for the Formation of Amino Indanes. With ammonia, 0.0369 g (2.75×10^{-4} mol) of **3** was mixed with 2 mL of a 1.4 M solution of ammonia to give a final concentration of 0.138 M. With methoxylamine, 0.021 g (1.56×10^{-4} mol) of oxide was added to 2 mL of a 1 M methoxylamine solution. Both reactions were allowed to proceed for 4 days. The reactions were worked up by adjusting the pH to 8, extracting with ether, drying the ethereal solution over anhydrous magnesium sulfate, and concentrating the solution in vacuo. The retention time (GLC) of the reaction products was compared to the retention times for known samples of 4- and 5-indanol and 4-[13] and 5-aminoindan. No detectable amounts of amino indans were found.

High-Pressure Liquid Chromatography Analysis. Arene oxide **3** was added directly to the kinetic solution at pH 7.2–7.6 and 15 min was allowed to lapse before the first injection was made (this time allowed for **3** → **4**). Injections were made into the HPLC after this every 30 min until the reaction reached ca. 5 half-lives. The HPLC analysis with detector at 275 nm showed the presence of only two product peaks at all pHs studied with 3-quinuclidinone, glycinamide, and phosphate buffer. By comparison with authentic samples of **10** and **11** (275 nm), the first peak to come off the HPLC was identified as 4-indanol (**10**) and the second peak as 5-indanol (**11**). Owing to the anomalous behavior of hydrazine seen in the kinetic runs, the infinity point solutions for the kinetic runs with hydrazine were also analyzed by HPLC and, again, only 4- and 5-indanol were observed.

Arene oxide **8** was added directly to kinetic medium at pH 0 (1 M HCl) and the reaction allowed to proceed to completion. Setting the detector at 282 nm and comparing with authentic samples of the α and β isomers of 5,6,7,8-tetrahydronaphthol (**12** and **13**, respectively), the α isomer came off first with the β isomer being detectable and coming off second.

Spectrophotometric Analysis. The extinction coefficients of **10** in acid at 275 and 270 nm in base are 558 and 270 M^{-1} cm^{-1}, respectively, and at 285 and 240 nm the extinction coefficients are 2453 and 8775 M^{-1} cm^{-1}, respectively. The extinction coefficient of **11** at 275 nm in acid is 2330 M^{-1} cm^{-1} while at 285 and 240 nm in base they are 1990 and 7423 M^{-1} cm^{-1}, respectively. The ratio of products from the overall reactions of arene oxide **3** at pH 6.92 (phosphate buffer) and 14 (1.0 M KOH) was determined from the absolute optical densities at t_∞. After completion of solvolysis at pH 6.92 (ca. 3 pH units below pK of **10** and **11**), the absolute optical density (OD) was obtained and the pH adjusted to 14 with a known amount of concentrated potassium hydroxide where the absolute OD was then redetermined. From this data and the molar extinction coefficients of 4- and 5-indanol (**10** and **11**) in acid and base under the same conditions,

Scheme I

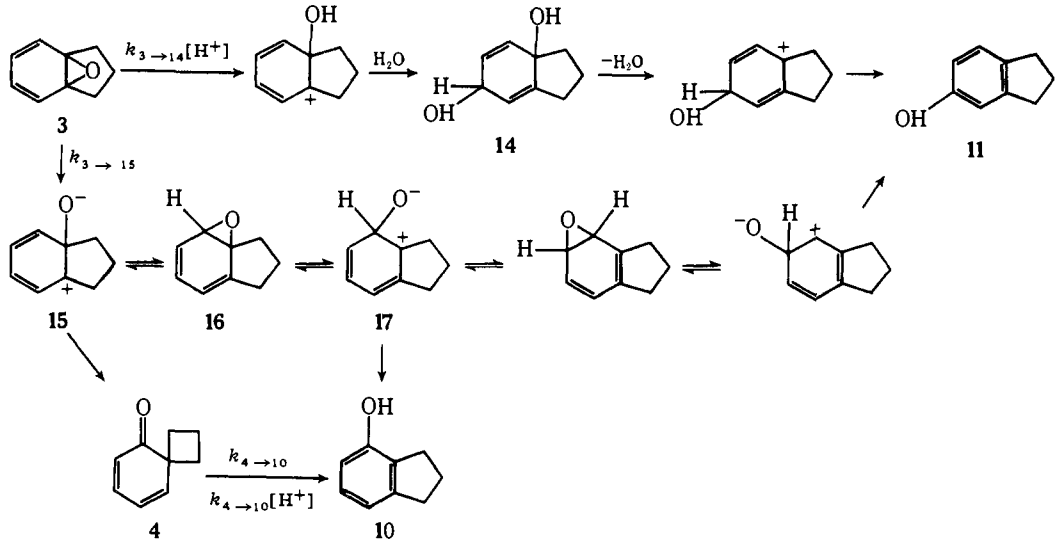

Table I. Comparison of the Rate Constants for Solvolysis of Arene Oxide **4** in 50/50 (v/v) Aqueous Dioxane[14] and Water

Rate constant[a]	Solvent 50/50 (v/v) H_2O–dioxane	Solvent H_2O	Ratio
$k_{3\rightarrow14}$, M^{-1} s^{-1}	1.4×10^3	2.7×10^4	19.3
$k_{3\rightarrow15}$, s^{-1}	1.4×10^{-3}	8.9×10^{-3}	6.4
$k_{4\rightarrow10}$ (base), s^{-1}	3.9×10^{-6}	1.0×10^{-4}	25.6
$k_{4\rightarrow10}$ (acid), M^{-1} s^{-1}	3.9	35.0	9.0

[a] For rate constants see Scheme I.

simultaneous equations were set up and solved for the concentration of the two products. The experiment at pH 14 was carried out in a similar manner except that a known amount of concentrated hydrochloric acid was added to adjust the pH to a value below 4 after the absolute OD was obtained at pH 14.

The concentration of **10** arising solely from dienone **4** at pH 14 was also determined. The OD at 240 nm (due to formation of anion of **10**) was obtained when the OD at 317 nm (due to formation of **4**) had reached a maximum (when all of **3** had reacted to yield **4**, **10**, and **11**). Then the ΔOD was obtained from the continued slower formation of **10** from **4**. This ΔOD, employing the determined extinction coefficient of **10** at 240 nm, yielded the percentage of product from the dienone–phenol rearrangement (**10** from **4**). Substracting this concentration of **10** from the final concentration of **10** and **11** determined from previous run at pH 14 using the same amount of **3** to initiate the reaction yielded the amount of **10** and **11** obtained directly from **3**.

The products from the reaction at 9,10-tetralin oxide (**8**) in acid were determined in the same manner as for 8,9-indan oxide (**3**). The extinction coefficients for **12** in acid at 285 and 275 nm were 59 and 987 M^{-1} cm^{-1}, respectively, while in base at 290 and 240 nm the extinction coefficients were 2837 and 7693 M^{-1} cm^{-1}, respectively. The extinction coefficients for **13** in acid at 285 and 275 nm were 1746 and 1824 M^{-1} cm^{-1}, while in base at 290 and 240 nm the extinction coefficients were 2510 and 7430 M^{-1} cm^{-1}, respectively. Owing to the rapid rate of solvolysis of **8**, only the product ratio at the end of the overall reaction could be determined.

pK_a Determinations. The pK_as of the phenolic products from reactions of dienones **5** and **9** were determined by a computer fit of ultraviolet spectral absorbances at pH values to a normal titration curve. At completion of reaction ca. 25 mL of the kinetic solution was transferred to the thermostated cell designed for the Cary 15[12] and, with nitrogen flowing over the top of the solution, the OD was determined as a function of pH at 30 °C. The pK_as of authentic samples of **6**, **12**, and **13** were also determined for comparison (see Results).

Results

Because spiro[3.5]nona-6,8-dien-5-one (**4**), the dienone of major interest in this study, is generated by rearrangement of 8,9-indan oxide (**3**), the solvolysis of the latter was reinvestigated in the course of the present study. The reaction sequence of Scheme I (with a minor revision from the present study) was elaborated previously.[14] A comparison of the rate constants determined in this study (H_2O solvent) and the previous study (50% v/v aqueous dioxane) is presented in Table I. By HPLC analysis, **4** produces only **10** at all pHs while **11** arises from **3** at basic pH via an oxygen walk from **15**. At the end of the reaction where **3** → **4**, ultraviolet spectral analysis employing determined extinction coefficients established that **3** yields **10** and **11** in the ratio 82 (±1):18 (±1), respectively. This ratio changes to 86 (±1):14 (±1), respectively, when all **4** has disappeared. In aqueous dioxane (50% v/v) there was obtained[14] at most only 3% of **11** in the basic pH region. The total concentration of **10** and **11**, when all of **4** has disappeared, is 95% of the starting concentration of **3**. The ratio of products **10** and **11**, which arise from **3** by way of **17** and **4**, was calculated to be 7.7:1, respectively (this ratio compares with 2.4:1 in 50% aqueous dioxane).[14]

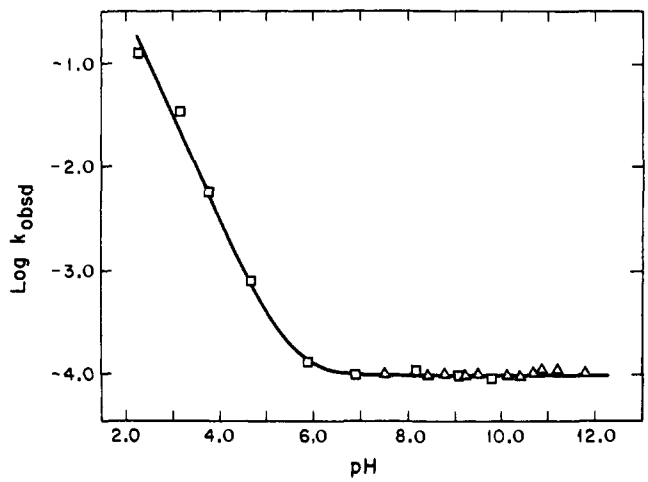

Figure 1. Plot of log k_{obsd} vs. pH for disappearance of **4** at 30 °C, μ = 1.0. The line was generated from eq 1. The squares represent data obtained from a pH-stat while the triangles represent data obtained from buffer dilution plots with amine buffers at $[N_T] = 0$.

A plot of the logarithm of the observed pseudo-first-order rate constant (k_{obsd}) vs. pH for the *rearrangement of spiro[3.5]nona-6,8-dien-5-one* (**4**) is shown in Figure 1 (30 °C, H_2O, μ = 1.0). The theoretical line through the points was generated from

$$k_{obsd} = 35a_H\ s^{-1} + 1.0 \times 10^{-4}\ s^{-1} \quad (1)$$

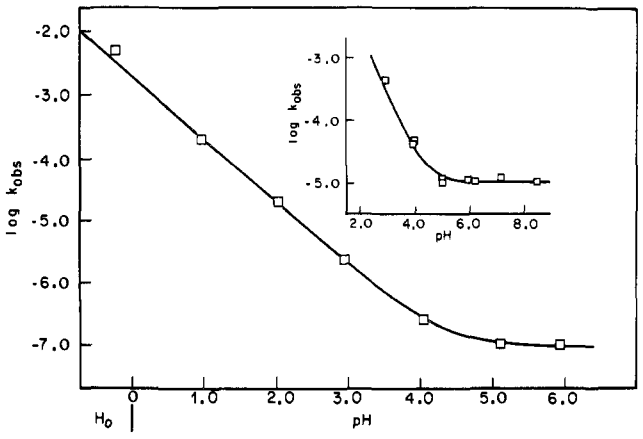

Figure 2. Plot of log k_{obsd} vs. pH (H_0 below pH 0) for disappearance of **5** at 30 and 78 °C (inset), respectively, μ = 1.0. The lines were generated from eq 2 and 3, respectively.

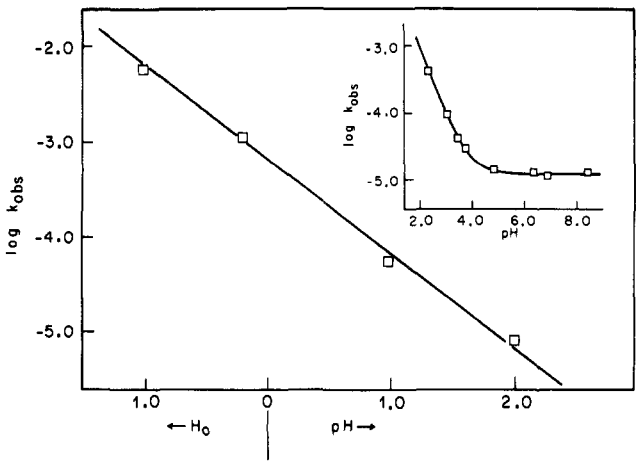

Figure 3. Plot of log k_{obsd} vs. pH (H_0 below pH 0) for disappearance of **9** at 30 and 83 °C (inset), respectively. The data points at 30 °C are fitted to a line generated from an equation containing only a specific acid term (see text) while 3b was generated from eq 4.

where a_H is the hydrogen ion activity determined at the glass electrode. The spontaneous rate for rearrangement of **4** at μ = 0.10 was found to be 8.64 ± 0.21 × 10^{-5} s^{-1} from an average of the k_{obsd} values obtained at pHs 6.81, 9.60, and 10.55. Reactions carried out in phosphate buffer (0.4 and 0.2 M, pH 6.48, μ = 1.0) proved identical with those determined in the absence of buffer. An increase in phosphate buffer concentration (0.24, 0.54, 0.84, and 1.2 M, pH 6.69, μ = 3.0) was accompanied by a depression in k_{obsd}. Therefore, the dienone–phenol rearrangement of **4** to **10** is not subject to general acid catalysis. A similar lack of buffer catalysis with carbonate–bicarbonate buffer (0.01–0.09 M, pH 9.57, μ = 1.0) was observed. The approximate enthalpies of activation were calculated ($\Delta H^{\ddagger}$ for k_H = 5.6 kcal/mol, $\Delta H^{\ddagger}$ for k_0 = 20.0 kcal/mol) from the two point plots (30.0 and 41.1 °C) of ln k vs. 1/K.

The log k_{obsd}–pH profiles for the *rearrangement of 6-benzyl-6-methyl-2,4-cyclohexadienone* (**5**) at 30 and 78 °C are shown in Figure 2. The theoretical line through the points in Fig. 2 was generated from

$$k_{obsd} = 2.0 \times 10^{-3}\, a_H\ s^{-1} + 1.0 \times 10^{-7}\ s^{-1} \qquad (2)$$

That a spontaneous reaction occurs at 30 °C is substantiated by the results at 78 °C (Figure 2, inset). The theoretical line through these points was generated from

$$k_{obsd} = 2.7 \times 10^{-1}\, a_H\ s^{-1} + 1.05 \times 10^{-5}\ s^{-1} \qquad (3)$$

The spontaneous rate at 83 °C was found to be 1.26 ± 0.11 × 10^{-5} s^{-1} (determined as the average of the rate constants obtained at pHs 6.88 and 8.43). The pK_a and λ_{max}s in acid and base of the product 2-benzyl-6-methylphenol (**6**) formed at all pHs and temperatures studied were identical with those values for authentic **6** (pK_a = 10.34 determined at 290 and 240 nm; for λ_{max}s see Experimental Section), the expected product in both the acid-catalyzed and spontaneous pathways.[9] From a three-point plot for k_0 (30, 75, and 83 °C) and a two-point plot for k_H (30 and 75 °C) of ln k vs. 1/K approximate enthalpies of activation were determined ($\Delta H^{\ddagger}$ for k_H = 21.8 kcal/mol, $\Delta H^{\ddagger}$ for k_0 = 19.4 kcal/mol). Buffer dilutions at 75 °C using acetate (0.02, 0.04, 0.1, and 0.2 M, pHs 3.94 and 5.01), phosphate (0.02, 0.04, 0.1, 0.2 M, pHs 6.18 and 6.86), and Tris (0.01, 0.04, 0.1, and 0.2 M, at pH 8.46) showed no buffer catalysis. No catalysis for rearrangement of **5** to **6** was seen with hydroxylamine or with trimethyl- or dimethylamine buffers at 30 °C.

The log k_{obsd}–pH profiles for the *rearrangement of spiro[4.5]deca-7,9-dien-6-one* (**9**) at 30 and 83 °C are shown in Figure 3. The rate constant for H_3O^+-catalyzed rearrangement at 30 °C was determined to be k_H = 5.6 × 10^{-4} M^{-1} s^{-1}. The theoretical line which best fits the data at 83 °C was derived from

$$k_{obsd} = 0.104 a_H\ s^{-1} + 1.20 \times 10^{-5}\ s^{-1} \qquad (4)$$

The rate constant for spontaneous rearrangement of **9** at 75 °C was also determined (5.36 ± 0.19 × 10^{-6} s^{-1}). The approximate enthalpies of activation were calculated ($\Delta H^{\ddagger}$ for k_H = 20.5 kcal/mol, $\Delta H^{\ddagger}$ for k_0 = 19.4 kcal/mol) from two-point plots of ln k vs. 1/K for both k_H (30 and 83 °C) and k_0 (75 and 83 °C). Buffer dilution studies with acetate, phosphate, and Tris at 83 °C and with hydroxylamine at 30 °C showed the rearrangement of **9** not to be subject to general or nucleophilic catalysis. The pK_a and λ_{max}s in acid and base of the product, at all pHs and temperatures studied, were identical with those of authentic 5,6,7,8-tetrahydro-1-naphthol (**12**) (pK_a = 10.27 at 290 and 240 nm; λ_{max} in acid at 276 and 269 nm, in base at 287 and 241 nm). The same product was obtained by Wiesel[7] under various conditions (Al_2O_3, *p*-toluenesulfonic acid in ether and 10% aqueous $HClO_4$). However, when the spent solutions from kinetic runs at pH −0.2 (1.0 M HCl,[4] 30 °C) and pH 6.88 (83 °C) were subjected to HPLC analysis (see Experimental Section), a small peak was observed with a greater retention time than that of phenol **12**. This peak had the same retention time as did an authentic sample of 5,6,7,8-tetrahydro-2-naphthol (**13**). By employing solutions of authentic **12** and **13** of the same total concentration as substrate in the kinetic run and comparing the integrated elution peaks to that of products **12** and **13** it could be shown that **9** produced ca. 0.25–0.50% of phenol **13** by both the acid-catalyzed and spontaneous pathways.

Owing to the slowness of the *rearrangement of 6,6-dimethyl-2,4-cyclohexadienone* (**7**), only its acid-catalyzed pathway of rearrangement could be obtained. The log k_{obsd}–pH profile at 30 °C is shown in Figure 4. The theoretical line which best fits the data points was derived from

$$k_{obsd} = 2.5 \times 10^{-3} \frac{a_H}{K_{aD} + a_H}\ s^{-1} \qquad (5)$$

where K_{aD} equals 3.98 × 10^{-4}. The rearrangement of dienone **7** has been studied under acid conditions (acetic anhydride with H_2SO_4 (catalyst) followed by hydrolysis)[9,10] and has been found to yield only 2,3-dimethylphenol (**18**). At 30 °C, **7** exhibited no reaction with either hydroxylamine or triethylamine buffers at concentrations up to 0.8 M in amine base.

Amine catalysis of the dienone–phenol rearrangement of 4 was shown in an experiment where **3** was added separately to

Table II. Rate Constants for the Reaction of Amines with **4** at 30 °, μ = 1.0

No.	Amine	pK_a[a]	pH range	No. of k_{obsd}	k_N M^{-1} s^{-1}	k_a, M^{-1} s^{-1}
1	Pyrrolidine	11.32	11.92–10.72	15	1.70×10^{-3}	
2	Piperidine	11.23	11.82–10.67	15	1.04×10^{-3}	
3	Quinuclidine	11.08	12.26–10.55	15	1.83×10^{-3}	
4	Ethylamine	10.72	11.95–10.16	25	2.46×10^{-4}	5.43×10^{-5}
5	*N*-Methylpiperidine	10.29	10.91–9.70	25	2.33×10^{-4}	1.67×10^{-4}
6	Allylamine	9.84	10.33–9.32	25	2.95×10^{-4}	8.73×10^{-5}
7	Trimethylamine	9.76	10.73–9.60	15	1.29×10^{-3}	
8	Glycine	9.63	10.55–9.18	10	2.15×10^{-4}	(2.24×10^{-5})[b]
9	Ammonia	9.21	11.70–9.87	15	2.46×10^{-5}	
10	3-Chloroquinuclidine	8.93	9.53–8.33	15	2.36×10^{-3}	
11	Hydrazine	8.15	8.46–7.88	20	1.78×10^{-3}	3.25×10^{-3}
12	Tris	8.14	8.82–7.55	25	2.09×10^{-5}	1.14×10^{-5}
13	Glycinamide	8.13	8.78–7.45	15	1.72×10^{-4}	(6.03×10^{-6})[b]
14	3-Quinuclidinone	7.49	8.14–6.90	15	2.06×10^{-3}	
15	Hydroxylamine	5.97	5.89–4.53	15	1.76×10^{-2}	

[a] Determined by half-neutralization. [b] Intercepts are close to zero and therefore these are approximate values.

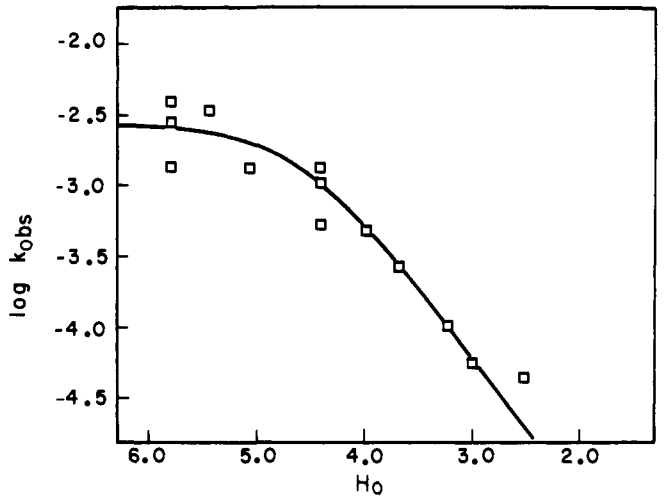

Figure 4. Plot of log k_{obsd} vs. H_0 for disappearance of **7** at 30 °C. The line was generated from eq 5.

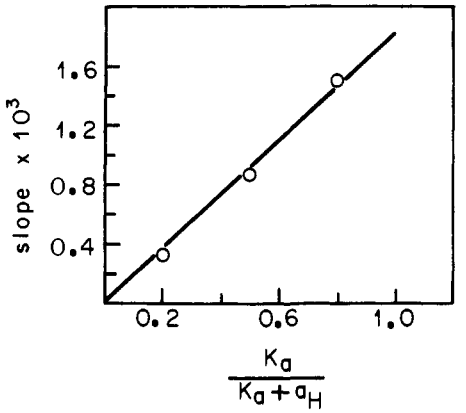

Figure 5. Plot of primary slopes (see text) vs. $K_a/(K_a + a_H)$ for reaction of **4** with pyrrolidine at 30 °C, μ = 1.0, at pHs 10.72, 11.32, and 11.92. The slope yields k_N.

glycine buffer and bicarbonate-carbonate buffer (pH 10.5) and the ensuing reactions followed at 317 nm. The formation of **4** was found to have the same rate constant in both buffers. The rate constant for disappearance of **4** was, however, greater in the amine buffer. The kinetics of reaction of amines with **4** were studied under pseudo-first-order conditions of total amine $[N_T]$ (= [NH] + [N]) ≫ [substrate].

$$k_{obsd} - k_{hydr} = k_N \frac{K_a}{K_a + a_H} [N_T] \quad (6)$$

Equation 6 is of the general form for those amines showing the simplest kinetic behavior where K_a refers to the acid dissociation constant of [NH] and k_{hydr} refers to the sum of $k_H a_H + k_0$ at a particular pH. Apparent second-order rate constants (k_N') were obtained from plots of $k_{obsd} - k_{hydr}$ vs. $[N_T]$ at a minimum of three pH values. A plot of these slopes (primary slope) vs. $K_a/(K_a + a_H)$ provides the second-order rate constant k_N as the slope (secondary slope) with the intercept equal to zero. A typical plot is shown for pyrrolidine in Figure 5. A listing of the derived rate constants is provided in Table II. Amines whose catalysis of rearrangement of **4** follow the kinetic expression of eq 6 include pyrrolidine, piperidine, quinuclidine, trimethylamine, ammonia, 3-chloroquinuclidine, and 3-quinuclidinone. For some amines, plots of the primary slopes vs. $K_a/(K_a + a_H)$ yielded nonzero intercepts. For these amines

$$k_{obsd} - k_{hydr} = \left(k_N \frac{K_a}{K_a + a_H} + k_a \frac{a_H}{K_a + a_H}\right) [N_T] \quad (7)$$

was found to apply. Defining the apparent second-order rate constant k_N' as $(k_{obsd} - k_{hydr})/[N_T]$ provides

$$k_N' / \frac{a_H}{(K_a + a_H)} = k_N \frac{K_a}{a_H} + k_a \quad (8)$$

A plot of $k_N'/a_H/(K_a + a_H)$ vs. K_a/a_H yields k_N as slope and k_a as the intercept. A typical plot is shown for allylamine in Figure 6. This type of behavior was found for ethylamine, *N*-methylpiperidine, allylamine, glycine, Tris, and glycinamide.

Plots of $k_{obsd} - k_{hydr}$ vs. $[N_T]$ for the α effector hydrazine exhibited upward curvature. However, a plot of $(k_{obsd} - k_{hydr})/[N_T]$ vs. $[N_T]$ was found to be linear (Figure 7). The kinetic behavior of hydrazine may be accounted for by

$$k_{obsd} - k_{hydr} = [N_T]^2 \left\{k_{NN} \left(\frac{K_a}{K_a + a_H}\right)^2 + k_{NH} \frac{K_a a_H}{(K_a + a_H)^2}\right\} + [N_T] \left(k_N \frac{K_a}{(K_a + a_H)} + \frac{k_a a_H}{K_a + a_H}\right) \quad (9)$$

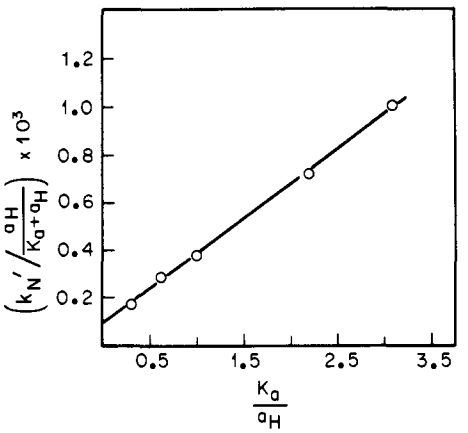

Figure 6. Plot of primary slopes/$a_H/(K_a + a_H)$ vs. K_a/a_H for reaction of **4** with allylamine at 30 °C, μ = 1.0, at pHs 9.32, 9.55, 9.84, 10.13, and 10.33. The slope yields k_N with the intercept equal to k_a.

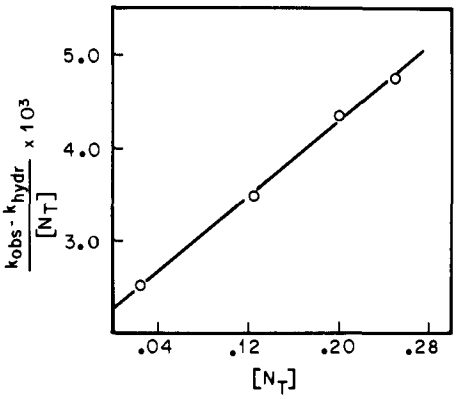

Figure 7. Plot of $(k_{obsd} - k_{hydr})/[N_T]$ for reaction of **4** with hydrazine at 30 °C, μ = 1.0, at pHs 7.88, 8.11, and 8.46. The slope yields $k_{NN'} + k_{NH'}$ with the intercept equal to $k_N' + k_a'$.

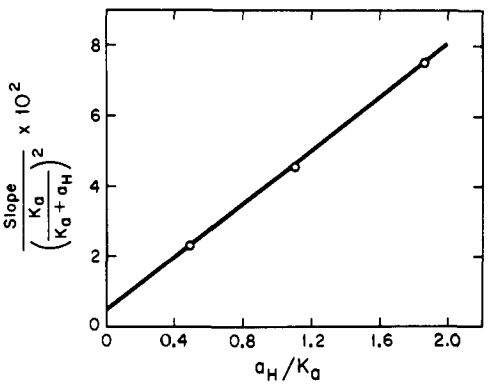

Figure 8. Plot of $(k_{NN'} + k_{NH'})/(K_a/(K_a + a_H))^2$ vs. a_H/K_a (see text) for reaction of **4** with hydrazine at 30 °C, μ = 1.0. The slope yields k_{NH} with the intercept equal to k_{NN}.

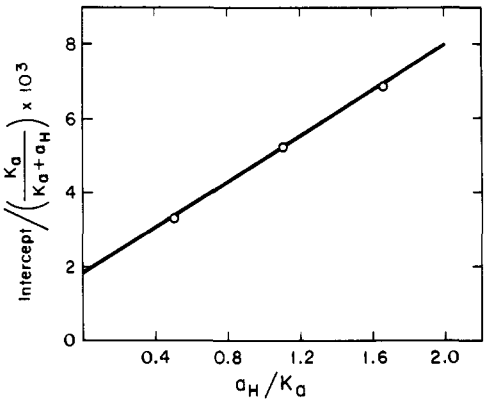

Figure 9. Plot of $((k_N' + k_a')/K_a)/(K_a + a_H)$ vs. a_H/K_a (see text) for reaction of **4** with hydrazine at 30 °C, μ = 1.0. The slope yields k_a with the intercept equal to k_N.

Dividing eq 9 by $[N_T]$ and plotting the left hand vs. $[N_T]$ yields the sum of the apparent pH-dependent third-order rate constant $(k_{NN'} + k_{NH'})$ as the slope with the intercept equal to the pH-dependent second-order rate constant $(k_N' + k_a')$. Dividing $(k_{NN'} + k_{NH'})$ by $(K_a/(K_a + a_H))^2$ and plotting vs. a_H/K_a yields k_{NH} as the slope with k_{NN} as the intercept (Figure 8). Dividing $(k_N' + k_a')$ by $K_a/(K_a + a_H)$ and plotting vs. a_H/K_a yields k_a as the slope and k_N as the intercept (Figure 9).

A scan from 350 nm to ca. 240 nm at the infinity point of each kinetic run for each amine at each pH used in this study always showed the λ_{max}s of the phenolic products (**10** and **11**). The products and their ratio were the same as seen in the absence of amine buffer as shown by UV product analysis with ethylamine (see Experimental Section) and HPLC analysis with 3-quinuclidinone, glycinamide, and hydrazine. This observation is in accord with **3** → **4** + **10** + **11** followed by **4** → **10** as seen in the absence of amine (Scheme I). The disappearance of **4** (317 nm) was found equal to the appearance of products (290 nm) on a dual wavelength spectrophotometer using ethylamine as the buffer. Bronsted plots of k_N and k_a are shown in plot A of Figures 10 and 11, respectively. Reactions on a preparative scale between **4** and both ammonia and methoxylamine failed to provide evidence for the formation of either 4- or 5-aminoindans (VPC, Experimental Section). Analysis by HPLC at infinity of kinetic runs with 3-quinuclidinone and glycinamide showed only peaks due to phenols **10** and **11**. Thus, the evidence indicates that aminoindans are not formed during the rearrangement of **4**.

The reaction of hydroxylamine with **4** (μ = 0.2) showed different behavior from the other amines at higher pH. The log k_{obsd} vs. pH profile for this reaction at constant $[N_T]$ is shown in Figure 12. The line which best fits the experimental points is given by

$$k_{obsd} - k_{hydr} = [N_T]\left\{\frac{k_1 K_a a_H + k_2 K_a K_w}{(K_a + a_H)a_H}\right\} \quad (10)$$

where K_a refers to the acid dissociation constant of HON^+H_3, and k_1 and k_2 the rate constants for attack by free hydroxylamine and specific base catalyzed attack of hydroxylamine. The values used to obtain the fit of the data points of Figure 12 follow: $k_0 = 1.0 \times 10^{-4}$ s^{-1}, $k_H = 19$ M^{-1} s^{-1}, $k_1 = 0.021$ M^{-1} s^{-1}, $k_2 = 1.5$ M^{-2} s^{-1}, $K_a = 5.27 \times 10^{-7}$, $K_w = 1.48 \times 10^{-14}$, and $[N_T] = 0.13$ M.

Discussion

The acid-catalyzed dienone-phenol rearrangement has long been recognized as a classical A-1 mechanism.[15a,b] However, in addition to the A-1 mechanism, there exists a non-acid-, non-base-catalyzed rearrangement which Miller has chosen to call a thermal rearrangement.[15b] His studies of thermal rearrangements have been carried out in apolar aprotic solvents at temperatures frequently exceeding 100 °C. As can be seen from this study (H_2O solvent) the dienones investigated (with the exception of **7**) were found to rearrange by both the acid-catalyzed and thermal or spontaneous pathways (Figures 1, 2b, and 3b). The pH corresponding to a transition from first to zero order in hydronium ion was dependent upon the dienone. Because of the lack of facility in the rearrangement of **7**, the reaction of this dienone was not followed at a high enough pH to observe spontaneous rearrangement.

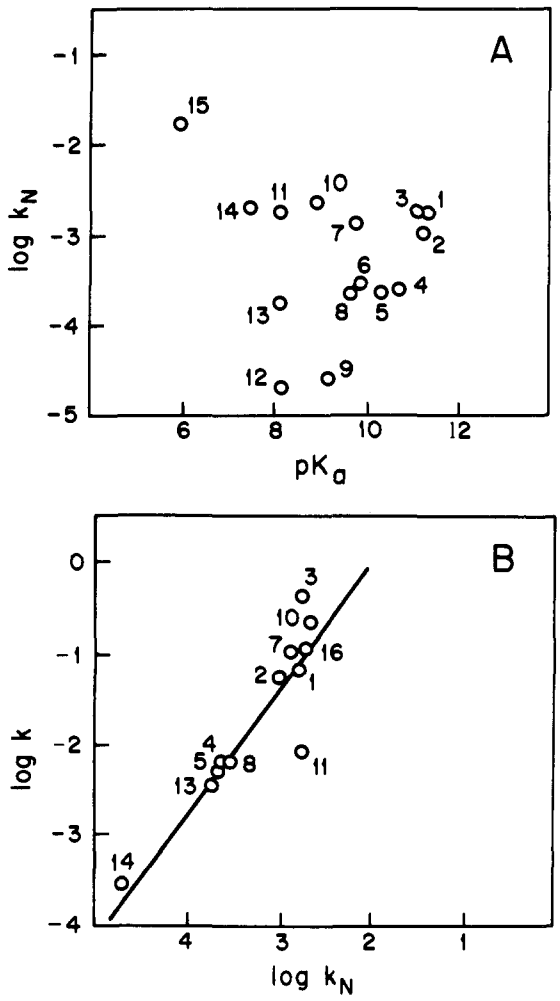

Figure 10. (A) Plot of log k_N (see text) vs. pK_a for reaction of amines with **4** at 30°, μ = 1.0. (B) Plot of log k for reaction of amines with 9,10-phenathrene oxide[16] vs. log k_N from this study, both at 30 °C, μ, = 1.0.

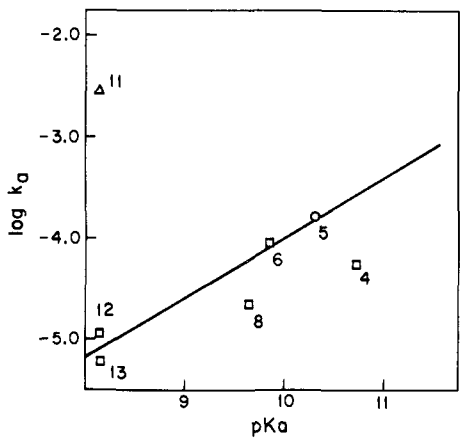

Figure 11. Plot of log k_a (see text) vs. pK_a for reactions of amines with **4** at 30 °C, μ = 1.0.

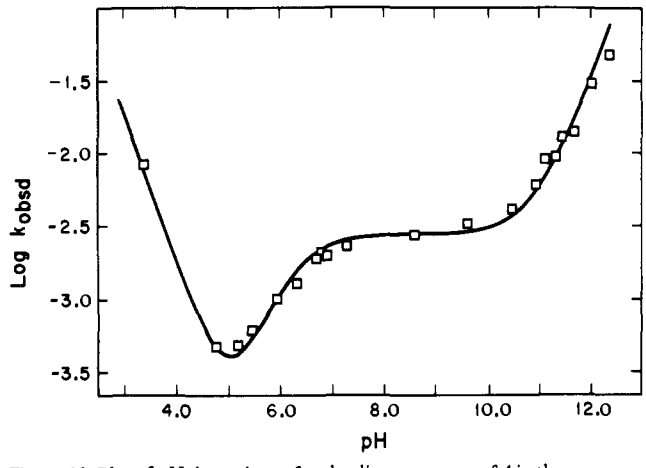

Figure 12. Plot of pH dependence for the disappearance of **4** in the presence of 0.13 M NH_2OH_T (= $^+NH_3OH + NH_2OH + NH_2O^-$) at 30 °C, μ = 0.2. The line was generated from eq 10.

The pseudo-first-order rate constant (k_{obsd}) for an A-1 mechanism can be expressed by

$$k_{obsd} = \frac{k_H a_H}{K_{aD} + a_H} \qquad (11)$$

(where K_{aD} is the acid dissociation constant of protonated dienone). The data points of Figure 4 have been fit to the line by employing eq 11 and pK_{aD} = −4.6 for protonated **7**. To the authors' knowledge this represents the first pK_{aD} value for a protonated linear conjugated dienone. Vitullo has reported a pK_{aD} of −3.7[16] on the H_0 acidity scale for the analogous but cross-conjugated dienone, 4,4-dimethyl-2,5-cyclohexadienone. Waring and co-workers[17a,b] have shown that cross-conjugated dienones may follow best the H_A acidity scale or may fall between the H_A and H_0 scale, or in a few examples the H_0 scale is followed most closely. That the data we obtained fit an equation employing a slope of −1.0 seems to support the use of the H_0 scale for **7**.

Clearly ring strain is responsible for the facile rearrangement of **4**. Thus, an increase in ring size on going from the spirocyclobutyl dienone (**4**) to the spirocyclopentyl dienone (**9**) results in a decrease of ca. $10^{4.8}$ in k_H. For the spontaneous rearrangement of the methylene moiety in **4** the rate constant exceeds that for benzyl migration in **5** by 10^3. Although not as large as in **4**, some ring strain also exists in **9**. This is shown by the fact that methylene group migration with **9** is almost as facile as benzyl group migration in **5**. It is recalled that the benzyl group is a better migrating group than an alkyl substituent.[18]

General acid catalysis could not be detected for the rearrangement of any of the dienones of this study. In the rearrangements of arene oxides to phenols, Bruice and Bruice[19] found that the specific acid and spontaneous pathways represented the extreme limits of a general acid pathway. General acid catalysis was found at pH values where H_3O^+ and "spontaneous" or water-catalyzed rearrangement are competitive. We also looked for general acid catalysis in the pH range where spontaneous and specific acid catalyzed dienone rearrangements are competitive, but could find no evidence for its existence. On cursory examination, spontaneous and acid-catalyzed arene oxide and 1,2-shift dienone rearrangements appear comparable if it is assumed that formation of carbonium ions (D, eq 12 and 13) are rate controlling. That general acid catalysis is not seen in the dienone rearrangement may be attributed to the large free-energy barrier for conversion of the carbonium ion C to dienone A (eq 13). In eq 12 and 13, HA refers to H_3O^+, water, and buffer acid. For arene oxide rearrangement the transition state for H_3O^+ catalysis lies close to the B → D reaction coordinate while for H_2O catalysis the transition state lies close to the C → D reaction coordinate.[19] Since the H_3O^+-catalyzed dienone–phenol rearrangement is an A-1 mechanism the transition state may be found along the B → D edge. The similarities of mechanism do not carry over to the spontaneous rearrangement, however. In the arene oxide case, the ring closure accompanying C → A is very facile. However, for the dienone rearrangement C → A must be associated with a sizable free-energy barrier, particularly for the rearrangement of **4** and **9**. On the other hand, protonation of

Table III. Estimated pK_as for Intermediates Derived from Either 1,2- or 1,4-Amine Attack, Respectively, on **4**[a]

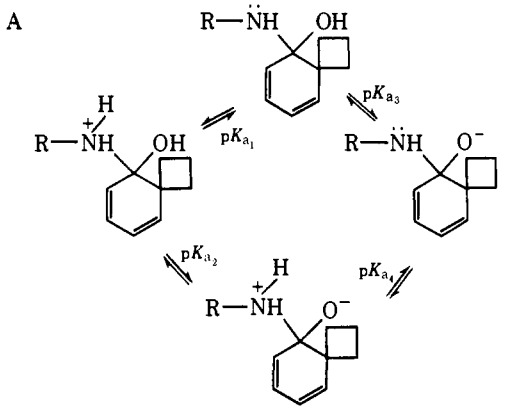

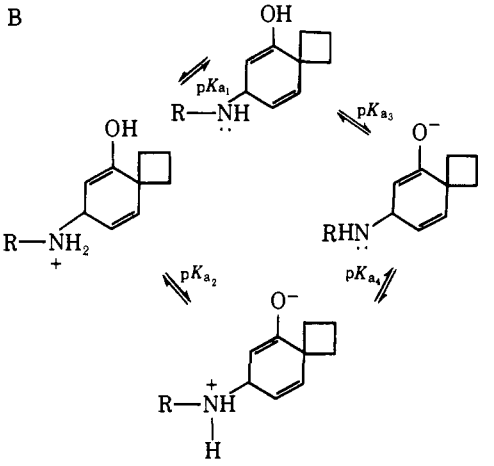

No.	pK_{a_1}	pK_{a_2}	pK_{a_3}	pK_{a_4}	pK_{a_1}	pK_{a_2}	pK_{a_3}	pK_{a_4}
1	9.5	10.6	15.9	14.8	12.5	11.9 → 12.0	12.2 → 12.3	12.7
2	9.6	10.6	15.9	14.9	12.4	11.9 → 12.0	12.2 → 12.3	12.6
3		10.3	15.9			11.9 → 12.0	12.2 → 12.3	
4	10.2	11.4	15.9	14.7	10.4	11.9 → 12.0	12.2 → 12.3	10.6
5		10.3	15.9			11.9 → 12.0	12.2 → 12.3	
6	9.4	11.4	15.9	13.9	9.7	11.9 → 12.0	12.2 → 12.3	9.9
7		10.3	15.9			11.9 → 12.0	12.2 → 12.3	
8	9.3	11.4	15.9	13.8	9.6	11.9 → 12.0	12.2 → 12.3	9.8
9	9.5	11.4	15.9	14.0	9.5	11.9 → 12.0	12.2 → 12.3	9.7
10		10.3	15.9			11.9 → 12.0	12.2 → 12.3	
11	7.8		15.5		8.1	11.9 → 12.0	12.2 → 12.3	8.3
12	7.8	11.0	15.7	12.5	8.1	11.9 → 12.0	12.2 → 12.3	8.3
13	7.8	11.0	15.7	12.5	8.1	11.9 → 12.0	12.2 → 12.3	8.3
14		10.3	15.9			11.9 → 12.0	12.2 → 12.3	
15	5.5		15.2		5.8	11.9 → 12.0	12.2 → 12.3	6.0

[a] See text. The number refers to the amine listed in Table II.

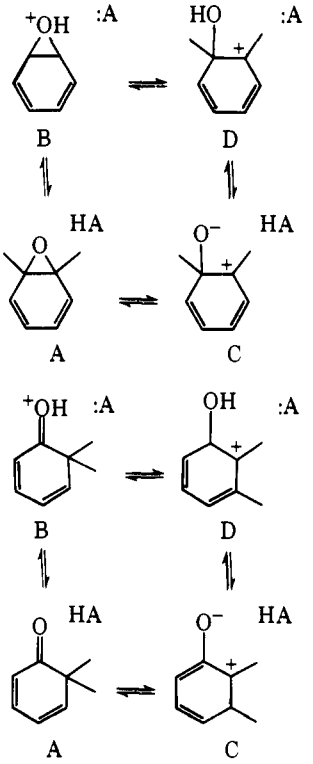

(12)

(13)

the zwitterion of C should be diffusion controlled. For these reasons proton transfer to the zwitterion in the spontaneous reaction of dienone (HA = H_2O) would not be even partially rate determining. The same consideration would hold when HA = general acid. One other consideration may be important. Since the spontaneous dienone-phenol rearrangement occurs in apolar aprotic solvents (benzene, etc.),[15b] the zwitterion C may go to phenol directly without passing through the carbonium ion D (by loss of H^+) or a suprafacial proton transfer may be involved in converting C → D. Data do not exist which allow a determination as to whether the thermal rearrangement in apolar aprotic solvents[15b] is, in detail, identical with the spontaneous rearrangement in H_2O. We surmise that it probably is.

Perhaps of most significance in this study was the finding of a facile catalysis by amines of the dienone-phenol rearrangement employing dienone **4**. The rearrangement of dienone **4** to phenol **10** was found to be catalyzed by all classes of aliphatic amines (see Table II). Nucleophilic catalysis can be logically envisioned with the attack step involving either 1,2-attack at the carbonyl carbon (formation of carbinolamine) or 1,4-attack at the C-3 carbon (Michael addition). Although the following schemes will show 1,4-attack, 1,2-attack will yield identical kinetic expressions. The question of 1,2- vs. 1,4-attack will be discussed later in this text.

Protonation of the carbonyl oxygen of **4** by H_3O^+ concerted with amine addition can be ruled out because this would require water as a general acid in the k_N term. The pK_{aD} of **4** can be estimated to be near −4.6 (kinetic pK_{aD} of similarity substituted **7** is −4.6). Employing the method of Fox and Jencks[20] (see Tables IIIA and IIIB) the pK_a of the intermediate (pK_{a2}) derived from 1,2-attack varies from 10 to 11 while for 1,4-attack it is ca. 12. Since the pK_a of water is ca. 15.7 at 30 °C general acid catalysis by water would be a violation of the libido rule.[21] In addition, amine catalysis has not been found to be assisted by buffer.

Scheme II

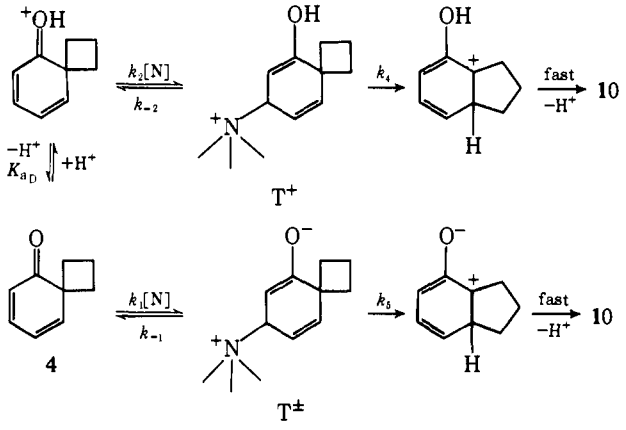

Scheme III

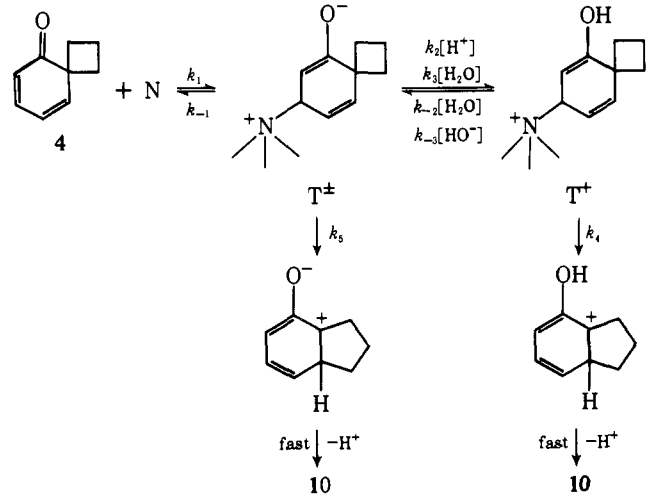

Competing nucleophilic attack upon **4** and protonated **4** in rate-determining steps may be considered (Scheme II with k_1 and k_2 rate determining). The assumption of preequilibrium protonation of **4** yields

$$k_{obsd} - k_{hydr} = [N_T]\frac{K_a}{K_a + a_H}\left\{\frac{k_1 a_H}{K_{aD} + a_H} + \frac{k_2 K_{aD}}{K_{aD} + a_H}\right\} \quad (14)$$

Since $K_{aD} \simeq 4 \times 10^4 \gg a_H$, eq 14 reduces to

$$k_{obsd} - k_{hydr} = [N_T]\frac{a_H}{K_a + a_H}\left\{\frac{k_1 K_a}{K_{aD}} + k_2\frac{K_a}{a_H}\right\} \quad (15)$$

which is kinetically equivalent to eq 8 with $k_N = k_2$ and $k_a = k_1 K_a / K_{aD}$. Using ethylamine (Table II) and substituting the experimentally determined constants k_a, K_a, and the estimated K_{aD}, a rate constant of 10^{11} s^{-1} is obtained for k_1. Within experimental error this number is equal to or greater than diffusion-controlled proton transfer from H_3O^+ and exceeds that for amine diffusion so that this scheme must be discarded.

An alternative to this scheme is obtained with the assumption of preequilibrium formation of **4**, protonated **4**, $T^{\pm}$, and T^+ followed by rate-determining migration (k_5 and k_4, Scheme II). Applying the above assumptions leads to eq 16 for k_{obsd}.

$$k_{obsd} - k_{hydr} = [N_T]\left\{\frac{k_5}{K_1}\frac{K_a}{K_{aD} + a_H}\frac{K_a}{K_a + a_H} + \frac{k_4}{K_2}\frac{a_H}{K_{aD} + a_H}\frac{K_a}{K_a + a_H}\right\} \quad (16)$$

Again assuming $K_{aD} \gg a_H$ eq 16 simplifies to

$$k_{obsd} - k_{hydr} = [N_T]\left\{\frac{K_a}{K_a + a_H}\frac{k_5}{K_1} + \frac{a_H}{K_a + a_H}\frac{k_4 K_a}{K_2 K_{aD}}\right\} \quad (17)$$

which is kinetically equivalent to eq 8 with $k_N = k_5/K_1$ and $k_a = k_4 K_a / K_2 K_{aD}$. Employing ethylamine and substituting for k_N, $k_5 = 2.5 \times 10^{-4} K_1$ while substituting for k_a, K_a, and estimated K_{aD}, $k_4 = 1.1 \times 10^{11} K_2$. In order for k_4 to have a realistic value (i.e., below diffusion control) K_2 ($= k_2/k_{-2}$) must have an upper limit of 10^{-2}. Since K_2 involves an equilibrium associated with the protonated dienone while K_1 ($= k_1/k_{-1}$) is associated with the neutral dienone we would expect K_2 to be several orders of magnitude larger than K_1. This sets an upper limit of 10^{-4} for K_1. Substituting this value for K_1 yields an upper limit for k_5 of 10^{-8}. Although we might have expected k_5 to be larger than k_4 (see later in Discussion), this scheme predicts that k_4 be larger than k_5 by ca. 10^{17}. This large difference and in the unexpected direction causes us to also discard this pathway.

Preequilibrium amine addition (Scheme III) to form intermediate $T^{\pm}$ which then goes on to product by partially rate-determining encounter-controlled proton transfer to T^+ in competition with departure of the amine from $T^{\pm}$ may be considered. Assuming steady-state concentrations of $T^{\pm}$ and T^+ leads to eq 18 for k_{obsd}.

$$k_{obsd} - k_{hydr} = [N_T]\frac{K_a}{K_a + a_H} \times \left\{\frac{k_1 k_5(k_{-2} + k_{-3}[HO^-] + k_4) + k_1 k_4(k_2 a_H + k_3)}{k_4(k_{-1} + k_2 a_H + k_3 + k_5) + (k_{-2} + k_{-3}[HO^-])(k_{-1} + k_5)}\right\} \quad (18)$$

For eq 18 to take on the form of eq 7 it is required that in the denominator $k_2 a_H < (k_{-1} + k_5)$. This requires, however, that $k_2 a_H$ be insignificant in the numerator and hence the protonation of $T^{\pm}$ to provide T^+ is unimportant; thus Scheme III is not kinetically competent.

The mechanism which best fits the experimental data is shown in Scheme IV. Assuming preequilibrium formation of $T^{\pm}$ and T^+ followed by rate-determining rearrangement concurrent with amine expulsion yields

$$k_{obsd} - k_{hydr} = [N_T]\frac{K_a}{K_a + a_H}\left\{\frac{k_{-1}k_5}{k_1} + \frac{k_{-1}k_4 a_H}{k_1 K_{aT}}\right\} \quad (19)$$

where all rate constants are as depicted in Scheme IV. Rearranging eq 19 provides

$$k_{obsd} - k_{hydr} = [N_T]\left\{\frac{k_{-1}k_5}{k_1}\frac{K_a}{K_a + a_H} + \frac{k_{-1}k_4 K_a}{k_1 K_{aT}}\frac{a_H}{K_a + a_H}\right\} \quad (20)$$

which is equivalent in form to eq 7 when $k_N = k_{-1}k_5/k_1$ and $k_a = k_{-1}k_4 K_a / k_1 K_{aT}$. The individual rate constants are not obtainable but the ratio $k_N/k_a = k_5 K_{aT}/k_4 K_a$. By substituting experimental values for k_N, k_a, and K_a and estimating K_{aT} for 1,2- and 1,4-attack (pK_{a2} of Tables IIIA and B, respectively) we can estimate the ratio k_5/k_4. For glycinamide k_5/k_4 for 1,2-attack is 2×10^3 while for 1,4-attack $k_5/k_4 = 2 \times 10^4$. For ethylamine $k_5/k_4 = 2.3$ for 1,2-attack while 1,4-attack yields 90. Thus, it appears that k_5 is always larger than k_4 (regardless of position of attack on **4**) with the relative difference increasing as the amine becomes a better leaving group (i.e., as the pK_a of the amine decreases). This indicates substantial departure of the amine in the transition state. One might predict $k_5 \gg k_4$ due to better stabilization of the developing positive charge at C-6 in the transition state (I) relative to

Scheme IV

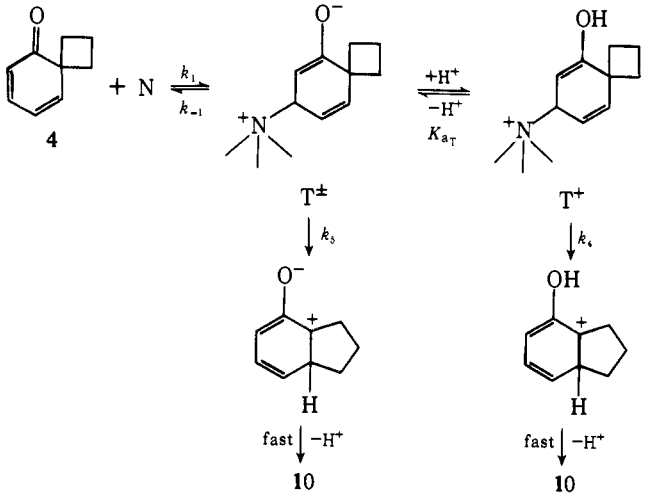

Scheme V

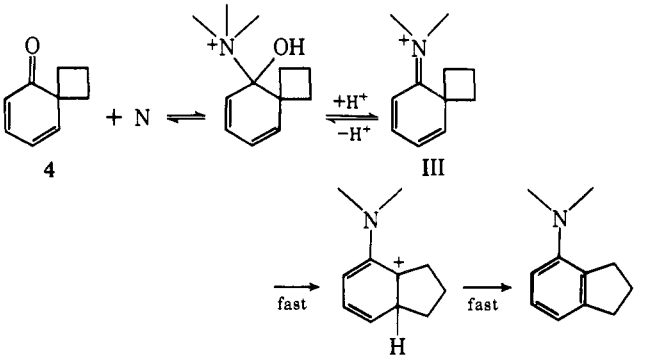

stabilization (perhaps inductive destabilization) by the hydroxyl group (II). Much the same consideration would apply

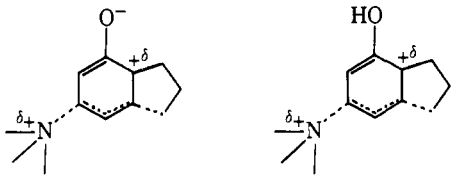

I II

to the intermediate obtained via 1,2-attack. If the nucleophilicity of the amine affects k_1/k_{-1} more than k_5 or k_4, the more nucleophilic the amine the larger would be the experimental k_N and k_a constants. As can be seen by the data (Table II), the α affectors hydroxylamine and hydrazine as well as the three quinuclidines gave the largest rate constants. In the quinuclidine series the three bonds to the nitrogen atom are bent back by the ring structure of the molecule such that the lone pair of electrons on the nitrogen should be readily available for nucleophilic attack and exhibit little steric crowding.[22] Their enhanced nucleophilicity (relative to their basicity) has also been found in the studies by Kallen and Jencks[23] on the reactions of amines with formaldehyde and by Bruice et al.[24] on nucleophilic displacement on arene oxides.

The question of 1,2- vs. 1,4-nucleophilic attack of amine preceding rearrangement of **4** may not be resolved with certainty. If 1,2-attack were involved, one might expect a linear correlation between the logarithm of the rate constants for amine-catalyzed rearrangement of **4** and the logarithm of the rate constants for amine attack on other carbonyl carbons. In such plots of log k_N vs. log k_N steric, electronic, and the α effects are normalized and a linear correlation is often obtained. Such correlations were not obtained when log k_N for reaction of amines with **4** were compared to log k_{nuc} for reaction of the same amines with trifluoroethyl thioacetate,[25] phenyl acetate,[26a,b] *p*-nitrophenyl acetate,[27] and 2,4-dinitrophenyl acetate.[26b] A reasonable correlation was obtained by use of the log k_N for amine attack on 9,10-phenanthrene oxide[24] (plot B of Figure 10). Here, nucleophilic attack is occurring on a saturated carbon atom of the oxirane ring of the arene oxide. The data of plot B of Figure 10 represents 12 amines and, with the exception of hydrazine and the three quinuclidines, a reasonable correlation is obtained. The slope of the best straight line through the data is ca. 1.2, which means that the change in rate for attack on **4** varies with the change in amine almost exactly as in the case of amine attack on 9,10-phenanthrene oxide. With the exception of hydroxylamine a good correlation was obtained when comparing log k_{nuc} for amine attack on methyl iodide to log k_N for rearrangement of **4**.[28] However, only five comparable data points are available. If 1,2-attack of amine upon **4** were occurring, the initially formed carbinolamine would be expected to be in equilibrium with the corresponding imine. The formation of protonated imine (III) as shown in Scheme V would in turn be expected to yield an aniline. Although anilines were looked for (see Results), none were found. These results lead us to favor 1,4-attack at C-3 of **4** over 1,2-attack at the carbonyl carbon of **4**. In the work of Langer et al.[29] on the reaction of dienone derivatives, i.e., *o*-benzoquinol acetates, with amines (ammonia, primary and secondary aliphatic, and primary aromatic amine) all products were the corresponding N-substituted *m*-aminophenols which arose from amine attack at C-3 with loss of acetic acid from C-6 with aromatization being the driving force for the reaction. For the dienone amine reactions of this study there is no leaving group at C-6, but, instead, an amine leaving group at C-3. The driving force for the reaction is not aromatization, but relief of strain, since aromatization does not occur in concert with alkyl group migration.

No real linear relationship of log k_a or log k_N to the pK_a of the conjugate acid of the amine nucleophiles is obtained for the rearrangement of **4**. Employing the few values of log k_a (Figure 11) a value of $\beta_{nuc} = 0.5$ is obtained. For the more numerous k_N values no correlation of log k_N and pK_a is obtained (plot A of Figure 10).

In addition to the paths through k_N and k_a, two of the amines (the α effectors hydroxylamine and hydrazine) exhibited additional reaction paths (see Results). The values of k_{obsd} for reaction of NH_2OH (0.13 M) with **4** as a function of pH are plotted in Figure 12. The plateau region seen in Figure 12 is above pH 7.5, a pH greater than the acid dissociation constant of $NH_3{}^+OH$(pK_{a1}), and represents catalysis by free hydroxylamine. Above pH 8 a rise in log k_{obsd} may be noted. We believe that this behavior is associated with the dissociation of NH_2OH to NH_2O^- (pK_{a2}) and is due to attack of the anion of hydroxylamine (NH_2O^-) on **4**. Since the value of $a_H \gg K_{a2}$ ($= 1.82 \times 10^{-14}$ at 25 °C[30]) the rate equation for disappearance of **4** in the presence of hydroxylamine should be given by

$$k_{obsd} - k_{hydr} = [N_T]\left\{\frac{k_1K_{a1}a_H + k_2K_{a1}K_{a2}}{(K_{a1} + a_H)a_H}\right\} \quad (21)$$

which is kinetically equivalent to the equation (10) employed to generate the plot of Figure 12. Hydroxylamine anion catalysis may occur through either oxy anion or nitrogen attack. Nitrogen attack is most reasonable since there is no evidence for catalysis by oxygen bases (catalysis of dienone–phenol rearrangement of **4** is not seen in 1.0 M KOH). With NH_2O^- the α effect would be enhanced over that in NH_2OH and this feature would, most importantly, increase the value of K_1 (Scheme IV).

The reaction of hydrazine is unusual in that two terms second order in hydrazine are obtained (eq 9), one equal to $[N]^2(k_{NN})$ and the other equal to $[N][NH](k_{NH})$. The de-

Scheme VI

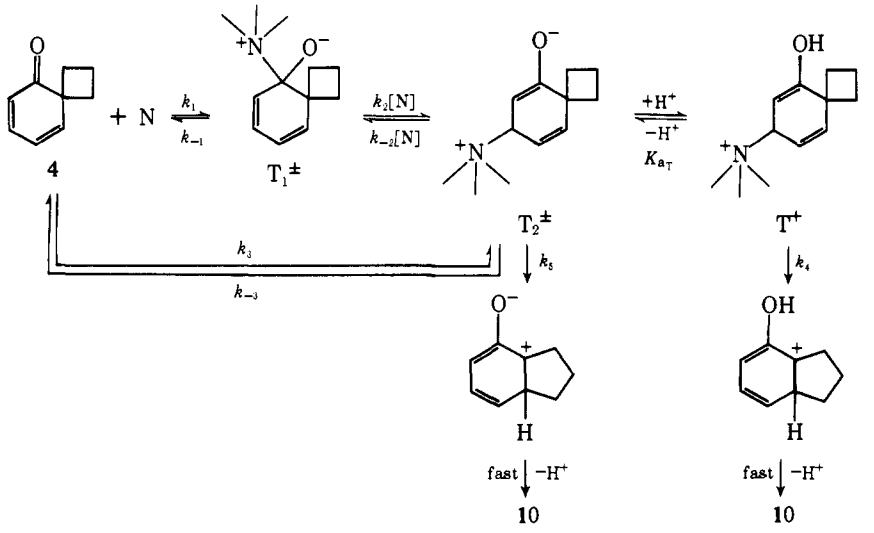

rived values of the rate constants are $k_{NN} = 4.2 \times 10^{-3}$ M^{-2} s^{-1} and $k_{NH} = 3.8 \times 10^{-2}$ M^{-2} s^{-1}. In addition both the k_N and k_a terms found with other amines are experimentally observed with hydrazine. A possible kinetic interpretation of hydrazine's behavior is shown in Scheme VI which involves 1,2-attack followed by 1,4-attack of hydrazine in competition with 1,4-attack. With the assumption of steady-state concentrations in $T_1^{\pm}$, $T_2^{\pm}$, and T^+, assuming $T_2^{\pm}$ and T^+ are in rapid equilibrium, and making the assumptions $k_{-1} > k_2[N]$ and $K_{aT}k_{-3} > K_{aT}(k_4 + k_{-2}[N]) + k_5a_H$ (all constants as shown in Scheme VI), one obtains

$$k_{obsd} - k_{hydr} = [N_T]^2 \left\{ \frac{K_1k_2k_5}{k_{-3}} \left(\frac{K_a}{K_a + a_H} \right)^2 + \frac{K_1k_2k_4K_a}{Ka_T} \frac{K_aa_H}{(K_a + a_H)^2} \right\} + [N_T] \left\{ K_3k_5 \frac{K_a}{K_a + a_H} + \frac{K_3k_4K_a}{K_{aT}} \frac{a_H}{K_a + a_H} \right\} \quad (22)$$

where $K_1 = k_1/k_{-1}$ and $K_3 = k_3/k_{-3}$. Equations 9 and 22 are kinetically equivalent so that $k_{NN} = K_1k_2k_5/k_{-3}$, $k_{NH} = K_1k_2k_4K_a/K_{aT}k_{-3}$, $k_N = K_3k_5$, and $k_a = K_3k_4K_a/K_{aT}$. Although the individual rate constants are not obtainable, this scheme predicts that $k_{NN}/k_{NH} = k_N/k_a$. Substituting the values given above, $k_{NN}/k_{NH} = 0.11$, while from Table II $k_N/k_a = 0.55$. Within the experimental error of the data and the methods employed in obtaining it the factor of 5 in the difference of the two ratios can be accepted in support of Scheme VI.

Acknowledgment. This work was supported by grants from the National Institutes of Health and the American Cancer Society.

References and Notes

(1) D. M. Johnson and T. C. Bruice, *J. Am. Chem. Soc.*, **97**, 6901 (1975).
(2) J. E. Tomaszewski, D. M. Jerina, and J. W. Daly, *Biochemistry*, **14**, 2024 (1975).
(3) P. Y. Bruice and T. C. Bruice, *J. Am. Chem. Soc.*, **98**, 844 (1976).
(4) Using the determined concentrations, the H_0 values for these solutions were obtained from data by M. A. Paul and F. A. Long, *Chem. Rev.*, **57**, 1 (1957).
(5) (a) J. Moschner, *Chem. Ber.*, **34**, 1258 (1901); (b) *ibid.*, **33**, 739 (1900); (c) E. Bamberger and M. Althausse, *ibid.*, **21**, 1893 (1888); (d) E. Bamberger, *ibid.*, **23**, 884 (1890).
(6) L. A. Paquett and J. H. Barrett, *Org. Synth.*, **49**, 62 (1973).
(7) M. Wiesel, Ph.D. Thesis, der Universitate Koln, 1966, p 61.
(8) D. Y. Curtin and M. Wilhelm, *J. Org. Chem.*, **23**, 9 (1958).
(9) B. Miller, *J. Am. Chem. Soc.*, **92**, 6252 (1970).
(10) E. N. Marvell and E. Magoon, *J. Am. Chem. Soc.*, **77**, 2542 (1955).
(11) V. P. Vitullo and M. J. Cashen, *Tetrahedron Lett.*, **48**, 4823 (1973).
(12) J. R. Maley and T. C. Bruice, *Anal. Biochem.*, **34**, 275 (1970).
(13) The 5-aminoindan was commercially available, but the chloride salt of the 4 isomer had to be prepared from reduction of 4-nitroindan with Raney nickel and hydrazine following the procedure of B. E. Leggetten and R. K. Brown, *Can. J. Chem.*, **38**, 2363 (1960).
(14) G. J. Kasperek, P. Y. Bruice, T. C. Bruice, H. Yagi, and D. M. Jerina, *J. Am. Chem. Soc.*, **95**, 6041 (1973).
(15) (a) A. J. Waring, *Adv. Alicyclic Chem.*, **1**, 207 (1966); (b) B. Miller, *Acc. Chem. Res.*, **8**, 245 (1975).
(16) V. P. Vitullo, *J. Org. Chem.*, **35**, 3976 (1970).
(17) (a) K. L. Cook and A. J. Waring, *J. Chem. Soc., Perkin Trans. 2*, 84 (1973); (b) M. J. Hughes and A. J. Waring, *ibid.*, 1043 (1974).
(18) A. Streitwieser, Jr., "Solvolytic Displacement Reactions", McGraw-Hill, New York, N.Y., 1962, p 74.
(19) P. Y. Bruice and T. C. Bruice, *J. Am. Chem. Soc.*, **98**, 2023 (1976).
(20) J. P. Fox and W. P. Jencks, *J. Am. Chem. Soc.*, **96**, 1436 (1974).
(21) W. P. Jencks, *J. Am. Chem. Soc.*, **94**, 4731 (1972).
(22) L. R. Fedor, T. C. Bruice, K. L. Kirk, and J. Meinwald, *J. Am. Chem. Soc.*, **88**, 108 (1966).
(23) R. G. Kallen and W. P. Jencks, *J. Biol. Chem.*, **241**, 5864 (1966).
(24) P. Y. Bruice, T. C. Bruice, H. Yagi, and D. M. Jerina, *J. Am. Chem. Soc.*, **98**, 2973 (1976).
(25) M. J. Gregory and T. C. Bruice, *J. Am. Chem. Soc.*, **89**, 2121 (1967).
(26) (a) T. C. Bruice, A. Donzel, R. W. Huffman, and A. R. Butler, *J. Am. Chem. Soc.*, **89**, 2106 (1967); (b) W. P. Jencks and J. Carriuolo, *ibid.*, **82**, 675 (1960).
(27) W. P. Jencks and M. Gilchrist, *J. Am. Chem. Soc.*, **90**, 2622 (1968).
(28) M. J. Gregory and T. C. Bruice, *J. Am. Chem. Soc.*, **89**, 4400 (1967).
(29) F. Langer, E. Zbiral, and F. Wessel, *Monatsh. Chem.*, **90**, 623 (1959).
(30) M. N. Hughes, H. G. Nicklin, and K. Shrimanker, *J. Chem. Soc. A*, 3485 (1971).